Disorder Induced Regular Dynamics in Oscillating Lattices

Thomas Wulf,[1,*] Benno Liebchen,[1] and Peter Schmelcher[1,2,†]
[1]Zentrum für Optische Quantentechnologien, Universität Hamburg, Luruper Chaussee 149, 22761 Hamburg, Germany
[2]The Hamburg Centre for Ultrafast Imaging, Universität Hamburg, Luruper Chaussee 149, 22761 Hamburg, Germany
(Received 27 August 2013; published 22 January 2014)

We explore the impact of weak disorder on the dynamics of classical particles in a periodically oscillating lattice. It is demonstrated that the disorder induces a hopping process from diffusive to regular motion; i.e., we observe the counterintuitive phenomenon that disorder leads to regular behavior. If the disorder is localized in a finite-sized part of the lattice, the described hopping causes initially diffusive particles to even accumulate in regular structures of the corresponding phase space. A hallmark of this accumulation is the emergence of pronounced peaks in the velocity distribution of particles that should be detectable in state of the art experiments, e.g., with cold atoms in optical lattices.

DOI: 10.1103/PhysRevLett.112.034101 PACS numbers: 05.45.Ac, 05.45.Pq, 05.60.Cd

Introduction.—Time-driven nonequilibrium dynamics is a subject of major interest [1–5], covering many different physical systems such as colloidal particles exposed to periodically modulated ion chains [6], particles moving along a filament with a hydrodynamic coupling to the surrounding solvent [7], or cold polar atoms loaded into optical lattices that are driven by periodic phase modulations of the applied laser beam [8–10]. A prototype example for a nonequilibrium phenomenon in driven lattices is the celebrated "ratchet effect," which is the appearance of directed particle motion in the absence of biased forces due to a breaking of certain spatiotemporal symmetries [11,12]. Whereas the aforementioned setups focus on globally acting time periodic forces, it was recently demonstrated how spatially varying ac forces introduce a plethora of effects [13–17] such as the formation of density waves [16], the patterned deposition of particles [15], or the possibility for conversion processes between diffusive and ballistic motion [16,17]. Moreover, long-range interactions have been shown to lead to dynamical current reversals in the absence of any parameter change [18]. In early works concerning disorder in complex systems, it was highlighted that in the presence of interactions and dissipation disorder may stabilize soliton solutions [19] or cause synchronization of coupled nonlinear oscillators [20]. In contrast, we demonstrate in the present Letter that the combination of disorder and driving in the absence of both interactions and dissipation can lead to the emergence of regular motion from an originally chaotic and diffusive ensemble of particles through a novel mechanism. Disorder-induced autocorrelations and pronounced changes of the velocity distributions are found with major differences occurring for the cases of global versus local disorder.

The driven lattice Hamiltonian.—We consider a one-dimensional lattice, consisting of laterally oscillating square barriers of width l and spacing L. Each barrier is labeled by an index $n_b \in \mathbb{Z}$ on which its potential height V depends, i.e., $V = V(n_b)$. The classical Hamiltonian for noninteracting particles is thus given by

$$H(x,p,t) = \frac{p^2}{2m} + \sum_{n_b=-\infty}^{\infty} V(n_b) \times \Theta(l/2 - |x - X_{0,n_b} - d(t)|), \tag{1}$$

where X_{0,n_b} is the equilibrium position of the n_bth barrier and $d(t) = A(\cos(\omega t) + \sin(2\omega t))$ is the driving law yielding directed transport [11,12]. We note that the effects and phenomena observed in this work do not rely on the specific shape of the lattice potential.

Disordered lattices can be realized by "perturbing" some barriers randomly, e.g., by setting $V(n_b) < V_0$ for some n_b. More precisely, we define a distribution $\sigma\colon n_b \in \mathbb{Z} \mapsto X \in (0,1)$, which assigns a random number to each barrier and determines its potential height via

$$V(n_b) = \begin{cases} V_0 - \eta\sigma(n_b), & \text{for } \sigma(n_b) \geq \gamma \text{ and } |n_b| < D \\ V_0, & \text{else} \end{cases} \tag{2}$$

where γ describes the relative amount of perturbed barriers, η controls the perturbation strength, and D accounts for the extension of the disorder region.

The focus of this work is on the regime of weak disorder that is accounted for by choosing $\gamma = 0.9$, and the remaining parameters are fixed to $m = V_0 = \omega = 1.0$, $L = 5.0$, $\eta = 0.9$, $A \approx 0.57$. Before we discuss the impact of disorder, let us briefly account for some of the main aspects of the dynamics in the uniformly driven lattice.

Dynamics in the unperturbed system.—The Hamiltonian given in Eqs. (1) and (2) contains the uniformly driven lattice with $V(n_b) \equiv V_0$ for all n_b by setting $D = 0$. As described in detail in Refs. [14,17], such a setup features a mixed phase space containing a "chaotic sea" at low kinetic energies that is bounded by invariant curves and shows

 © 2014 American Physical Society

regular islands embedded in the chaotic sea. The stroboscopic Poincaré surface of section, where at times $t = 2\pi n$ with $n \in \mathbb{N}$ velocity and position x modulus the barrier distance L are recorded, is shown in Fig. 1(a) for the parameters as mentioned above. Correspondingly, there are two distinguished types of motion apparent: Either a trajectory is located within the chaotic sea or it is located within any of the regular structures. Opposite to the diffusive motion in the chaotic sea the regular motion for islands above or below $v = 0$ preserves the sign of the particle velocity, i.e., $v(t)v(t + \Delta t) > 0$ for any t and Δt and corresponds to ballistic motion.

Dynamics in the disordered system.—We now demonstrate how the presence of disorder influences the previously described dynamics in the driven lattice. A suitable observable to distinguish between diffusive and ballistic motion is the autocorrelation function, which as we shall see below is altered significantly by the inclusion of disorder. Velocity distributions represent a second valuable tool to analyze the impact of disorder and are discussed afterwards. The velocity autocorrelation function (VACF)

$$A_j(k) = \frac{1}{k-j} \sum_{i=1}^{k-j} \frac{2 v_i v_{i+j}}{v_i^2 + v_{i+j}^2}, \qquad k > j \qquad (3)$$

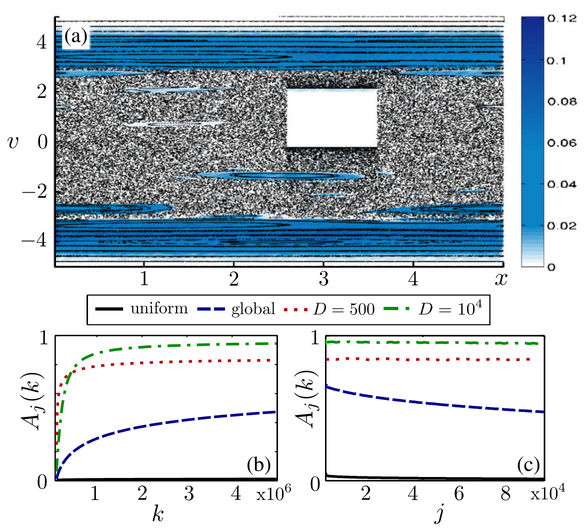

FIG. 1 (color online). (a) In black: stroboscopic Poincaré surface of section of a driven lattice without disorder. For parameters, see main text. Coloring: phase space occupation of an ensemble at $t = 10^6$ for localized disorder for $D = 10^4$. (We add the potential energy to particles within the barrier to avoid discontinuities, which causes the blank rectangle.) (b) Dependence of ensemble averaged VACFs $A_j(k)$ on the number of particle-barrier collisions k for $j = 10^5$. (c) VACF $A_j(k)$ as a function of j for $k = 5 \times 10^6$. Setups: uniform lattice (black straight line); global disorder (blue dashed line); localized disorder for $D = 500$ (red dotted line) and $D = 10^4$ (green dashed-dotted line).

relates the velocity of a particle after its ith collision v_i with its velocity after the $(i + j)$th collision with one of the barriers, and the normalization ensures that $-1 \leq A_j(k) \leq 1$. On the one hand, if a particle moves diffusively through the lattice, its velocity is allowed to switch its sign and different terms of the sum can cancel each other. On the other hand, if a particle moves ballistically, v_i and v_{i+j} have the same sign and, thus, the terms in Eq. (3) add up. Hence, $A_j(k)$ is a useful quantity to distinguish between ballistic and diffusive motion in the lattice. As a starting point, we calculate the ensemble averaged VACF numerically for the uniform setup, i.e., $D = 0$ in Eq. (2), for $j = 10^5$. For this purpose, we propagate in total 10^6 trajectories for 100 different disorder realizations $\sigma(n_b)$. The initial conditions are $x = 0$ and a randomly chosen velocity with $-0.1 < v_0 < 0.1$ to ensure that all trajectories are initially located within the chaotic sea of the unperturbed system. The resulting VACF is shown in Fig. 1(b) and can be seen to evolve with increasing collision number k to a small nonzero value. This is a consequence of the directed transport induced by the bichromatic driving, which is accompanied by an asymmetric chaotic sea with respect to $v = 0$ implying a drift of the diffusive chaotic motion (see Ref. [17] for details).

In the presence of global disorder, i.e., $D \to \infty$, we observe a much stronger increase of the VACF that is even more pronounced for the two setups with localized disorder, as shown for $D = 500$ and 10^4. Note that while the VACF appears to saturate for both locally disordered setups, there is no sign of saturation for the globally disordered lattice. To ensure that the different behavior in the cases of localized and global disorder is not an artifact of the particular choice of the delay j, we show additionally the VACFs for fixed $k = 5 \times 10^6$ as a function of j in Fig. 1(c). Apparently, the increase of $A_j(k)$ does not require any specific choice of the delay j but is present over the entire investigated parameter regime.

Let us now investigate how the velocity distributions of particle ensembles are influenced by the disorder. These distributions $\rho(v)$ were obtained by propagating particle ensembles in different setups containing globalized, localized, or no disorder with initial conditions as before. After a simulation time of $t = 10^6$, the velocity of each particle is recorded, yielding the distributions $\rho(v)$ as shown in Figs. 2(a)–2(c). For the uniformly driven lattice [Fig. 2(a)], we observe that all particles are confined within a velocity interval $-5 \lesssim v \lesssim +5$, and a further inspection reveals that after a certain transient time of $t \approx 10^4$, $\rho(v)$ becomes stationary. This behavior is easily understood by inspecting the phase space of the unperturbed system [Fig. 1(a)]: All particles are initially located within the chaotic sea and are occupying it uniformly after a transient time. Because the chaotic sea is bounded by invariant curves, the velocity distribution is bounded as well. The apparent dips in $\rho(v)$, e.g., at $v \approx -2$, are caused by regular islands, i.e., parts of

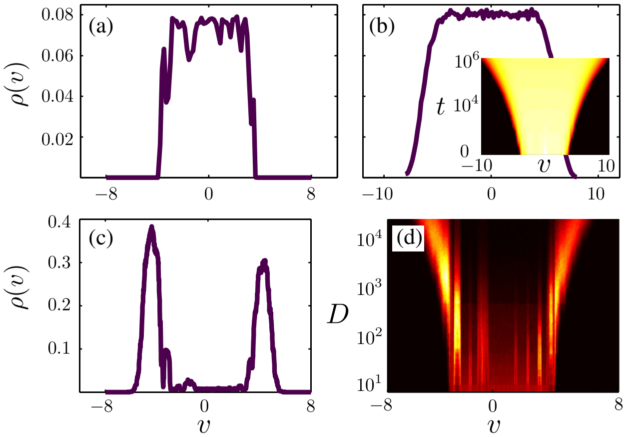

FIG. 2 (color online). Velocity distributions $\rho(v)$ at $t = 10^6$ for uniform driving (a), global disorder (b), and localized disorder with $D = 10^4$ (c). (d) Velocity distributions at $t = 10^6$ for disorder extension D between 10 and 5×10^4. The inset in (b) is the time evolution of $\rho(v)$ for the same setup as in (b) with logarithmic color scaling for better visibility.

the phase space that are prohibited for chaotic trajectories and, thus, lead to a reduced density of chaotic trajectories in these velocity intervals.

For the globally disordered lattice [cf. Fig. 2(b)], the pronounced dips as seen in Fig. 2(a) cease to exist. Moreover, the time evolution of $\rho(v)$ [inset of Fig. 2(b)] indicates that no stationary distribution is reached. On the contrary, $\rho(v)$ spreads to higher and higher velocities as time proceeds. In some sense, the effect of a broadening of the velocity distribution appears to be reversed for the setup of localized disorder with $D = 10^4$ [Fig. 2(c)] where we observe two pronounced peaks accompanied by smaller ones. Similar to the uniformly driven lattice, $\rho(v)$ reaches a stationary form after a transient time of approximately $t \approx 2 \times 10^5$. Finally, we show the asymptotic velocity distributions recorded at $t = 10^6$ when almost all particles have left the disorder region for different extensions of the disorder region ranging from $D = 10$ up to $D = 5 \times 10^4$ in Fig. 2(d). Already for small values of D the emergence of peaks is apparent and they become more populated by particles as compared to the background as D increases. At $D \gtrsim 10^2$ the peaks at small energies start to gradually disappear until at $D \gtrsim 10^4$ only the two dominant ones remain, which become broader and spread to higher energies as D is enlarged further.

Particle accumulation in regular islands.—Let us now explore the physical mechanism behind the observed impact of disorder on the velocity distributions as well as on the VACFs. We first discuss the case of global disorder and explain the differences to local disorder afterwards.

As argued above, the choice $\gamma = 0.1$ ensures that most barriers remain unperturbed. Hence, we can expect to gain insight into the dynamical processes of the disordered system by performing projections onto the phase space of the unperturbed system (PSUS). In the disorder-free lattice, trajectories belong either to the chaotic sea or to one of the regular islands for all times. In a system with weak disorder, the scattering of a particle off a barrier modified due to the disorder can be interpreted as a hopping process in the PSUS. The crucial observation is now that the corresponding shift in phase space may transport the particle from the chaotic sea onto a regular island of the PSUS, in which it is trapped until a further collision with a disorder barrier occurs and the particle may either reenter the chaotic sea or remain within the island. Such an island entering event is shown exemplarily in the inset of Fig. 3 where the velocity as a function of time is shown for a single trajectory. While the particle moves diffusively at early as well as at late times, it follows a quasiperiodic orbit of a regular island and, thus, moves ballistically for intermediate times. The fact that the velocity distributions for the globally disordered lattice [Fig. 2(b)] feature neither pronounced dips nor peaks suggests that at the time when $\rho(v)$ is recorded both the chaotic as well as the regular islands of the PSUS are populated uniformly. At the same time, particles can become faster than in the uniformly driven lattice by entering regular spanning curves at velocities above the chaotic sea. This leads to the spreading of $\rho(v)$ to increasingly higher velocities [as seen in the inset of Fig. 2(b)].

We now address the question why localized disorder both leads to peaked velocity distributions and increases the VACF. Figure 1(a), which shows the occupation of the phase space on top of the PSUS for the ensemble at $t = 10^6$ for localized disorder with $D = 10^4$, reveals that peaks in $\rho(v)$ as shown in Fig. 2(c) are caused by an accumulation of particles within regular structures of the phase space of the uniform part of the lattice. More precisely, the two dominant peaks correspond to particles on invariant

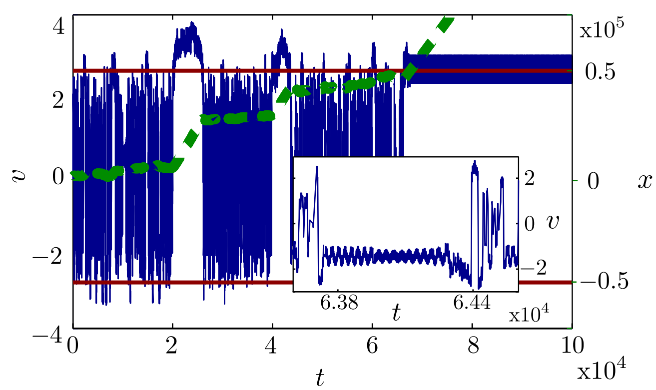

FIG. 3 (color online). Position (right ordinate, green dashed line) and velocity (left ordinate, blue line) as a function of time for a single trajectory. The horizontal red lines are at $x = \pm x_D = \pm 5 \times 10^4$ and delimit the region of disorder. The inset is a zoom into $v(t)$, indicating the entering and exiting processes of a quasiperiodic orbit.

spanning curves, whereas the smaller peaks are related to particles in regular islands of the PSUS. In the following, we identify two distinct mechanisms that both contribute to the observed accumulation in regular structures.

Multiple entering of disorder region: Apparently, the above described conversion processes from regular to chaotic motion or vice versa can only occur for particles that are still within the disorder region, that is, if $|x| < x_D \equiv DL$. Once the particle passes x_D, we have to distinguish two different scenarios: Either the particle passes x_D while being in a regular structure of the PSUS or it is located in the chaotic sea of the PSUS. In the former case, the particle does not reenter the disordered region and, thus, cannot leave its regular "host" because no further collisions with perturbed barriers occur. Such an event is shown in Fig. 3: The considered particle switches between diffusive and ballistic phases until it eventually reaches x_D within a regular structure of the PSUS. Afterward, the particle remains in the corresponding quasiperiodic orbit. If on the other hand the particle crosses the edge of the disorder region at x_D while being within the chaotic sea of the PSUS, it can cross this edge several times since the diffusive chaotic motion can transport the particle back to the position x_D. Accordingly, it has several chances of being transformed into a ballistic particle by means of a collision with a perturbed barrier. Thus, the possibility to cross the edge at x_D several times as long as the particle remains chaotic is one of the reasons why the majority of particles become regular in the lattices with localized finite disorder.

Separation of length scales: Consider a particle located near the center of the disorder region. As Fig. 3 illustrates, such a particle undergoes both diffusive as well as ballistic phases, whereas the average distance covered within a diffusive phase, denoted by l_d, is smaller than it is in a ballistic phase, because the former includes frequent changes in the sign of the velocity whereas the latter does not. Consequently, the probability that a particle reaches the edge of the disorder region x_D within a ballistic phase can be expected to be higher than it is for a diffusive phase. Hence, this separation of length scales leads to an accumulation of particles into regular structures of the PSUS if $x_D \gg l_d$, which is to a lower degree fulfilled for $D = 500$ as it is for $D = 10^4$ leading to a correspondingly lower value of the VACF. Note that because particles perform particularly long ballistic flights at high kinetic energies ($|v| \gtrsim 4$) this separation of length scales is the reason the two peaks in Fig. 2(c) at these high energies are the most prominent peaks.

Conclusions.—We have investigated the impact of disorder on the nonequilibrium dynamics of classical particles in a one-dimensional driven lattice. The disorder causes initially diffusive chaotic particles to enter regular regimes of the phase space. As hallmarks of these processes, we observed both the emergence of pronounced peaks in the velocity distribution of particle ensembles as well as synchronized particle motion if the disorder is localized in a finite region of the lattice. Since none of the presented phenomena requires any fine tuning of the system parameters and rely solely on the existence of a mixed phase space, we believe that our findings are of relevance in understanding the dynamics in different experimental setups such as cold atoms in optical lattices [8,10,21]. In these experiments counterpropagating laser beams, which are periodically phase modulated, provide a laterally driven quasi-one-dimensional lattice potential. By employing a large detuning between the laser field and the inner atomic transition, the Hamiltonian regime can be reached, and finally, disorder can be introduced by superimposing an optical speckle field, as was done, e.g., in Ref. [22].

Relating the above used parameters to experimentally relevant quantities yields, for a driven lattice experiment with cold rubidium atoms in an optical lattice, that the ratio of the driving frequency f and potential height V_0 should be $f^2/V_0 \sim 1(\mathrm{MHz}/E_r)$ where E_r is the recoil energy. A possible realization would be $f = 10$ MHz and $V_0 = 100E_r$, which are similar to the parameters that have been used in Ref. [10], and thus, we believe that disorder-induced regular behavior and the associated peaks in the velocity distribution can be observed specifically in cold atom but also in other setups.

*Thomas.Wulf@physnet.uni-hamburg.de
†Peter.Schmelcher@physnet.uni-hamburg.de

[1] T. Salger, S. Kling, T. Hecking, C. Geckeler, L. Morales-Molina, and M. Weitz, Science **326**, 1241 (2009).
[2] P. Hänggi and F. Marchesoni, Rev. Mod. Phys. **81**, 387 (2009).
[3] S. Denisov, S. Flach, and P. Hänggi, Europhys. Lett. **74**, 588 (2006).
[4] J. Gong and P. Brumer, Phys. Rev. Lett. **97**, 240602 (2006).
[5] L. Wang, G. Benenti, G. Casati, and B. Li, Phys. Rev. Lett. **99**, 244101 (2007).
[6] S. Bleil, P. Reimann, and C. Bechinger, Phys. Rev. E **75**, 031117 (2007).
[7] P. Malgaretti, I. Pagonabarraga, and D. Frenkel, Phys. Rev. Lett. **109**, 168101 (2012).
[8] R. Gommers, S. Denisov, and F. Renzoni, Phys. Rev. Lett. **96**, 240604 (2006).
[9] P. Phoonthong, P. Douglas, A. Wickenbrock, and F. Renzoni, Phys. Rev. A **82**, 013406 (2010).
[10] A. Wickenbrock, P. C. Holz, N. A. A. Wahab, P. Phoonthong, D. Cubero, and F. Renzoni, Phys. Rev. Lett. **108**, 020603 (2012).
[11] S. Flach, O. Yevtushenko, and Y. Zolotaryuk, Phys. Rev. Lett. **84**, 2358 (2000).
[12] N. R. Quintero, J. A. Cuesta, and R. Alvarez-Nodarse, Phys. Rev. E **81**, 030102 (2010).
[13] P. Reimann and M. Evstigneev, Europhys. Lett. **78**, 50 004 (2007).

[14] C. Petri, F. Lenz, F. K. Diakonos, and P. Schmelcher, Phys. Rev. E **81**, 046219 (2010).

[15] B. Liebchen, C. Petri, F. Lenz, and P. Schmelcher, Europhys. Lett. **94**, 40 001 (2011).

[16] C. Petri, F. Lenz, B. Liebchen, F. K. Diakonos, and P. Schmelcher, Europhys. Lett. **95**, 30 005 (2011).

[17] T. Wulf, C. Petri, B. Liebchen, and P. Schmelcher, Phys. Rev. E **86**, 016201 (2012).

[18] B. Liebchen, F. K. Diakonos, and P. Schmelcher, New J. Phys. **14**, 103032 (2012).

[19] N. V. Alexeeva, I. V. Barashenkov, and G. P. Tsironis, Phys. Rev. Lett. **84**, 3053 (2000).

[20] Y. Braiman, J. F. Lindner, and W. L. Ditto, Nature (London) **378**, 465 (1995).

[21] R. Gommers, V. Lebedev, M. Brown, and F. Renzoni, Phys. Rev. Lett. **100**, 040603 (2008).

[22] M. White, M. Pasienski, D. McKay, S. Q. Zhou, D. Ceperley, and B. DeMarco, Phys. Rev. Lett. **102**, 055301 (2009).